Viscosity-Dependent Dynamics of CO Rebinding to Microperoxidase-8 in Glycerol/Water Solution

Jaeheung Park, Taegon Lee, and Manho Lim*

Department of Chemistry and Chemistry Institute of Functional Materials, Pusan National University, Busan, 609-735 Korea

Received: June 2, 2010; Revised Manuscript Received: July 15, 2010

Rebinding kinetics of CO to microperoxidase-8 (Mp), an excellent model system for the active site of heme proteins such as myoglobin and hemoglobin, was measured after photolysis of MpCO in solutions with various viscosities and temperatures, using femtosecond vibrational spectroscopy. Whereas the geminate rebinding of CO to Mp in water is negligible, significant fractions of CO rebind nonexponentially within 1 ns at room temperature in a glycerol/water solution. The geminate yield of the CO rebinding increases and its rate accelerates as the viscosity of the solution increases either by increasing glycerol content in glycerol/water mixtures at 294 K or by decreasing temperature of the solution from 323 to 283 K. The nonexponential rebinding kinetics can be described by the theory of a diffusion-controlled reaction and the data are well reproduced by the pair survival probability function in the absence of any interaction potential between the pair. The rebinding kinetics was also successfully described by the SRC model, a distributed linear coupling model for the CO rebinding.

Introduction

The rebinding of small ligands to heme proteins after photolysis has been widely studied as a model system for understanding how protein function is related to structure and dynamics.[1−3] The pioneering work by Frauenfelder and coworkers has shown that the rebinding of CO to myoglobin (Mb) at cryogenic temperatures is highly nonexponential and complex due to protein conformation inhomogeneity and/or conformational relaxation after deligation.[2,4−8] The rebinding kinetics of CO and NO to Mb in various viscosity solutions, as well as at various temperatures, had been further explored to extract the molecular level of details in protein conformational changes following deligation and its effect on ligand binding.[8−21] Ligand rebinding in heme proteins is complicated by possible ligand migration within the protein and escape into solution, as well as the presence of the protein conformational substate and its relaxation. Thus, the kinetics of ligand rebinding to bare heme, iron protoporphyrin IX (FePPIX), was comparatively investigated to determine the intrinsic ligand rebinding characteristics to heme molecules free from protein environments and conformational changes.[22−30]

Rebinding of CO to H_2O-FePPIX in solution was found to be nonexponential, even in the absence of protein conformational substates,[26,27,29,30] suggesting that the nonexponential rebinding kinetics of CO is an inherent property of the solvated heme and that the nonexponentiality observed in Mb does not necessarily require the presence of protein conformational substates.[29] The observed nonexponentiality in the bare heme was attributed to either the diffusion of CO[27] or a distribution of enthalpic barriers for the rebinding.[29,31] The theory of diffusion-influenced homogeneous reactions combined with the theory of isolated pairs was used to derive an analytical expression that successfully described the kinetics of CO rebinding to H_2O-FePPIX in a 79% glycerol/water (w/w) mixture at 260−300 K.[27] It was suggested that the diffusive motion of CO was solely responsible for the nonexponential rebinding of CO to the bare heme in solution.[27] The interconversion between inhomogeneous heme structures that may have different rebinding rates was assumed to be sufficiently fast in high-temperature solutions (260−300 K), and thus a single (averaged) rate for reaction at the heme was used.[27] Whereas the rebinding of CO to H_2O-FePPIX was temperature-dependent and nonexponential, that of NO to H_2O-FePPIX was found to be temperature-independent and exponential.[29] The diffusion model for ligand rebinding to the bare heme was revoked by arguing that exponential rebinding could not be explained by the diffusive motion of NO.[29] Instead, a distributed linear coupling model developed by Srajer, Remin, and Champion (SRC) was introduced to describe CO rebinding kinetics.[31] In the SRC model, the nonexponential kinetic behavior of CO arose from a distributed enthalpic barrier that fluctuates on time scales slower than the CO rebinding time. The distribution in the Fe out-of-plane displacement accompanying the heme doming after photolysis was suggested to be the main cause of nonexponential rebinding of CO to H_2O-FePPIX in an 80% glycerol/water (v/v) mixture within 40−293 K.[29]

The active heme in heme proteins is coordinated to a proximal histidine in its fifth coordination site. Clearly, the heme molecule with a proximal histidine such as 2-methlyimidazole-coordinated FePPIX (2MeIm-FePPIX) is a better-suited system for the active molecule in heme proteins. The rebinding of CO to 2MeIm-FePPIX showed much slower geminate rate and lower geminate rebinding yield than H_2O-FePPIX.[28,30] It was suggested that fluctuational averaging of the rebinding barrier was faster than the CO rebinding to 2MeIm-FePPIX and thus its CO rebinding was described by an exponential function.[30] However, we found that the small geminate yield in 2MeIm-FePPIX hampered any sophisticated modeling (other than an exponential function) for its CO rebinding kinetics and precluded clear differentiation between kinetics models.[28] As the diffusion model failed to describe the kinetics of NO rebinding, the SRC model also fell

* To whom correspondence should be addressed. E-mail: mhlim@pusan.ac.kr.

10.1021/jp1050436
Published on Web 08/04/2010

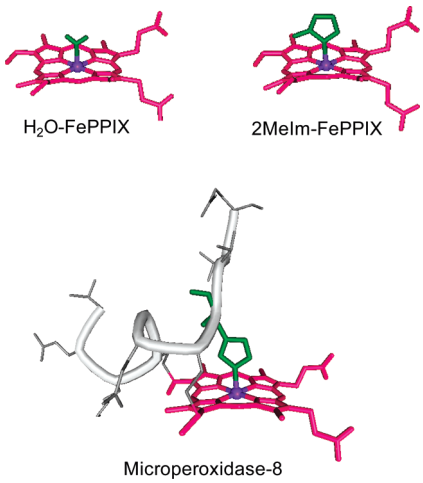

Figure 1. Structures of model hemes. Structure of microperoxidase-8 (Mp) is from that of horse heart ferri cytochrome *c* (Protein Data Bank entry 1HRC). Residual protein backbone in Mp is shown in a gray solid tube and peptide in gray lines. The proximal ligand is shown in green and the heme in purple. FePPIX: iron protoporphyrin IX; 2MeIm: 2-methylimidazole.

short describing the rebinding of NO with physically meaningful parameters. A harpoon mechanism was thus introduced to describe NO rebinding that decoupled with the heme conformation, resulting in exponential rebinding kinetics.[32]

Microperoxidase-8 (Mp), a fragment of cytochrome *c* consisting of a heme with an eight amino acid peptide covalently linked to a heme through a (proximal) histidine, was also used as a model system for the active molecule of the heme proteins.[33] MpCO, which has a necessary skeleton for the built-in proximal histidine, revealed much more efficient geminate rebinding than (proximal histidine mimicking) imidazole bound FePPIX-CO, with its geminate yield similar to that of H_2O-FePPIX, not 2MeIm-FePPIX. A global (networked) structure involving the proximal histidine (Figure 1), in addition to its presence, might be necessary for the characteristics of the active molecule in the heme proteins. Considering that the CO rebinding to 2MeIm-FePPIX was different from that of Mp, the CO rebinding to Mp should be addressed. Although Mp is an excellent model system mimicking the active molecule of the heme protein in the absence of a specifically organized distal pocket and protein conformational substates, a systematic investigation of ligand rebinding to Mp has not been carried out yet.

Herein, we measured CO rebinding to Mp in various viscous solutions near room temperature to obtain the reaction characteristics of the active molecule in heme proteins free from protein conformational substates and its relaxation after deligation. The geminate rebinding of CO to Mp is highly nonexponential with geminate yield increasing as the viscosity of the solution increased. The kinetic behavior of the CO can be well described by either the diffusion model or the SRC model.

Materials and Methods

The details of the time-resolved vibrational spectrometer used here are described elsewhere.[34] Briefly, two identical home-built optical parametric amplifiers (OPA), pumped by a commercial Ti:sapphire regenerative amplifier (Hurricane, Spectra Physics) with a repetition rate of 1 kHz, were used to generate a visible pump pulse[35] and a mid-IR probe pulse.[36,37] A pump pulse at 575 nm with 3.5 μJ of energy was generated by frequency doubling of a signal pulse of one OPA. A tunable mid-IR probe pulse was generated by difference frequency mixing of the signal and idler pulse of the other OPA. The polarization of the pump pulse was set at the magic angle (54.7°) relative to the probe pulse to recover the isotropic absorption spectrum. The broadband transmitted probe pulse was detected with a 64-element $N_2(l)$-cooled HgCdTe array detector. The array detector was mounted in the focal plane of a 320 mm monochromator with a 150 *l*/mm grating, resulting in a spectral resolution of ca. 1.4 cm^{-1}/pixel at 1960 cm^{-1}. The signals from each of the detector elements were amplified with a home-built 64-channel amplifier and digitized by a 12-bit analog-to-digital converter. Chopping the pump pulse at half the repetition frequency of the laser and computing the difference between the pumped and unpumped absorbances determined the pump-induced change in the absorbance of the sample (ΔA). Due to the excellent short-term stability of the IR light source (<0.3% rms), less than 1.0×10^{-4} rms in absorbance units after 0.5 s of signal averaging was routinely obtained without single shot referencing with an independent detector. The pump spot was made sufficiently larger than the probe spot to ensure spatially uniform photoexcitation across the spatial dimensions of the probe pulse. The instrument response function was typically 180 fs.

The Mp tends to aggregate in aqueous solution with the degree of aggregation critically depending upon pH, ligation, and the nature of the solvent.[33,38] For example, whereas 0.04 μM Mp starts to aggregate at pH 7, 32.5 μM Mp was found to be monomeric at pH 12.[33] For MpCO, a 50 μM sample was reported to be monomeric in aqueous solution.[39] Hydrophobic effects were found to be a main culprit for the aggregation.[40] Due to lower polarity, alcohol−water mixtures can generate higher concentration monomeric metalloporphyrins than water alone.[40] We also found that metalloporphyrins have a greater monomeric tendency in glycerol/water mixtures than in purely aqueous solutions.[28] Clearly, the tendency of aggregation is diminished by ligation of CO, higher pH, as well as a lowering dielectric constant of the solution. Thus, we prepared MpCO in an alkaline glycerol/water solution and maintained the concentration low enough to avoid sample aggregation. A 1−2 mM Mp stock solution was prepared by dissolving microperoxidase-8 (Sigma) in deoxygenated 1.0 M NaOD (Aldrich). The stock solution was diluted into an appropriate deoxygenated glycerol/water mixture, reduced with excess amounts of sodium dithionite (Aldrich), and ligated with CO by bubbling the gas for more than 10 min. The composition of the glycerol/water mixture was adjusted to change the viscosity of the MpCO sample.[41] The final MpCO sample pD was 12 and the concentration 50−100 μM. The sample was loaded into a gas-tight 100-μm-path length flowing sample cell with two 2-mm-thick CaF_2 windows. Monomeric MpCO was confirmed by UV−vis and IR spectra of the sample. The temperature of the cell was maintained within 1 K of the desired value by a circulating bath. Deuterated water (D_2O) was used to avoid overlap of the interested spectrum with strong water absorption bands.

Results

Figure 2 shows the vibrational band of the CO stretching mode of MpCO in viscous solutions at 294 K. The single-featured vibrational band in MpCO was blue-shifted from and broader than that in MbCO. The CO vibrational band in MpCO, well described by a Gaussian function centered at 1955 cm^{-1} with 24 cm^{-1} fwhm (full width at half-maximum), was similar to that of a typical model heme, 6-coordinated CO bound ferrous FePPIX such as 2MeIm-FePPIX-CO (at 1958 cm^{-1} with 28

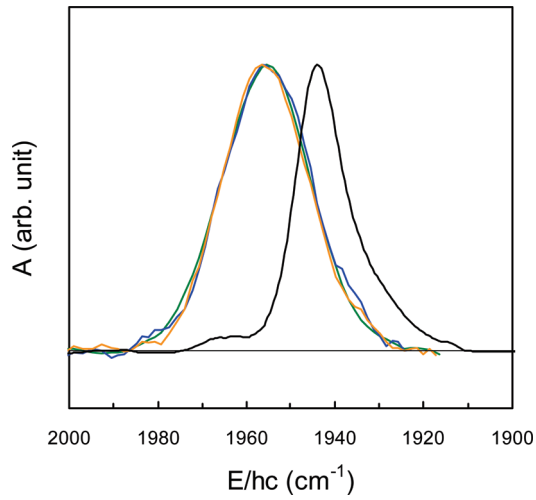

Figure 2. Normalized vibrational spectra of CO in MpCO in glycerol/water mixtures at 294 K. Glycerol content in water was 65.3% (18 cP, red line), 75.3% (53 cP, blue line), and 85.3% (127 cP, green line) by volume.[41] Data were obtained from time-resolved spectra at 0.3 ps pump−probe delay. The spectrum of MbCO in 58% glycerol/water (v/v) (black line) is also shown for comparison.

cm^{-1} fwhm)[28] and H_2O-FePPIX-CO (at 1955 cm^{-1} with 23 cm^{-1} fwhm).[30] Broader CO bands in MpCO likely arose from exposure of CO to inhomogeneous glycerol/water mixtures compared with the well-organized distal environments in MbCO with 8−12 cm^{-1} fwhm.[4,42] The CO band in aggregated MpCO would bear different characteristics from that in the monomer. Thus, if there were MpCO aggregates in the sample, the observed vibrational spectrum would possess several bands. The observed CO band is single-featured and independent of the glycerol content of the solution in the presented sample conditions (65−90% glycerol in volume), corroborating that the MpCO sample used in our experiment is indeed in a monomeric form.

Figure 3 shows transient vibrational spectra of the CO stretching mode of MpCO after photolysis of the heme molecule in 85% glycerol/water (v/v) at 294 K. The negative-going feature (bleach), characteristics of which are identical to the equilibrium IR spectrum of CO in MpCO, arises from the loss of bound CO. The magnitude of the initial bleach corresponded to ca. 20% photolysis of MpCO. The shape of the bleach spectra did not change with the pump−probe delay. The magnitude of the bleach represented the population of the deligated Mp at the given pump−probe delay. A great portion of the bleach was recovered in 1 ns, indicating that a significant fraction of the dissociated CO geminately rebinds in 1 ns. Bimolecular rebinding proceeds on the millisecond time scale,[27,30] much longer than the experimental time span of 1 ns. Thus, the decay within 1 ns could be attributed to geminate recombination and contribution from bimolecular rebinding will be neglected hereafter. To quantify the population change of the deligated Mp, the entire set of spectra was globally optimized with the Marquardt−Levenberg nonlinear least-squares fitting routine. In the fitting, whereas the center wavenumber and bandwidth of a Gaussian is globally optimized, the amplitude of the Gaussian was optimized at each time. The amplitude represents the survival fraction of the deligated Mp after photolysis of MpCO. The time-resolved spectra of MpCO in 85% glycerol/water (v/v) at various temperatures, as well as that in various glycerol/water mixtures and in D_2O at 294 K were also measured, from which the kinetics of the survival fraction of the deligated Mp at various solvent conditions was obtained

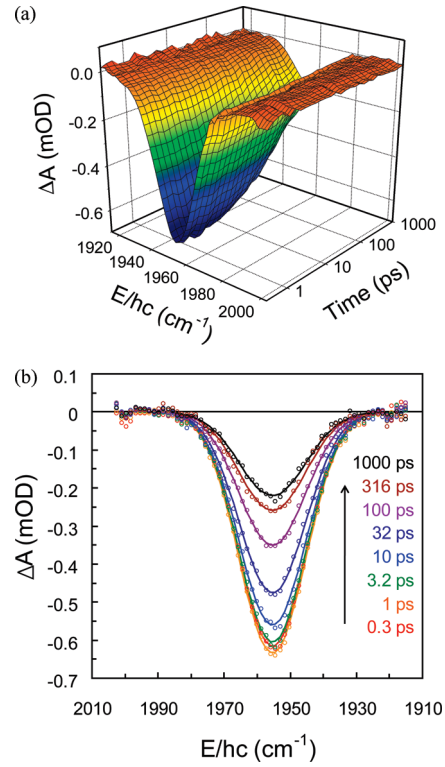

Figure 3. (a) Three-dimensional plot of time-resolved vibrational spectra of CO after photolysis of MpCO in 85% glycerol/water (v/v) at 294 K. (b) Representative spectra (open circles) are modeled with a Gaussian function centered at 1955 cm^{-1} with 24 cm^{-1} fwhm (solid lines). The units are the difference in optical density (OD, 1 mOD = 10^{-3} OD) between the samples after and before photolysis. The bleach signal arises from the loss of bound CO. For clarity, the quadratic polynomial modeling signal due to thermal contribution from the solvent has been subtracted from the measured spectra. Note that the delay time is in a logarithmic scale.

(Figure 4). As shown in Figure 4a, significant fractions of CO nonexponentially rebound to Mp in viscous glycerol/water mixtures within 1 ns, but there was no detectable rebinding of CO to Mp in D_2O up to 1 ns at 294 K, the experimental time window. Temperature-dependent kinetics for the survival fraction of the deligated Mp was very similar to that in a solution of corresponding viscosity at 294 K.[41]

The kinetics of the survival fraction of the deligated Mp was modeled by the pair survival probability function in the absence of any interaction potential between the pair; $W(t)$ was derived in the theory of the diffusion-influenced bimolecular reaction:[27,43,44]

$$W(t) = 1 - \frac{R}{r}\frac{k_0}{k_0 + k_D}[\Omega(B/\sqrt{t}) - \Omega(A\sqrt{t} + B/\sqrt{t})] \times \exp(-B^2/t) \quad (1)$$

$$A \equiv \left(1 + \frac{k_0}{k_D}\right)\frac{\sqrt{D}}{R}, \quad B \equiv \frac{r - R}{2\sqrt{D}}, \quad \Omega(x) \equiv \exp(x^2)\,\mathrm{erfc}(x)$$

$$\mathrm{erfc}(z) = \frac{2}{\sqrt{\pi}}\int_z^\infty \exp(-y^2)\,dy$$

$$k_D = 2\pi RD$$

where D is the relative diffusion coefficient of the reacting pair, r is the distance for the initial separation between them, R is the reaction radius, and k_0 is the intrinsic rate constant at the

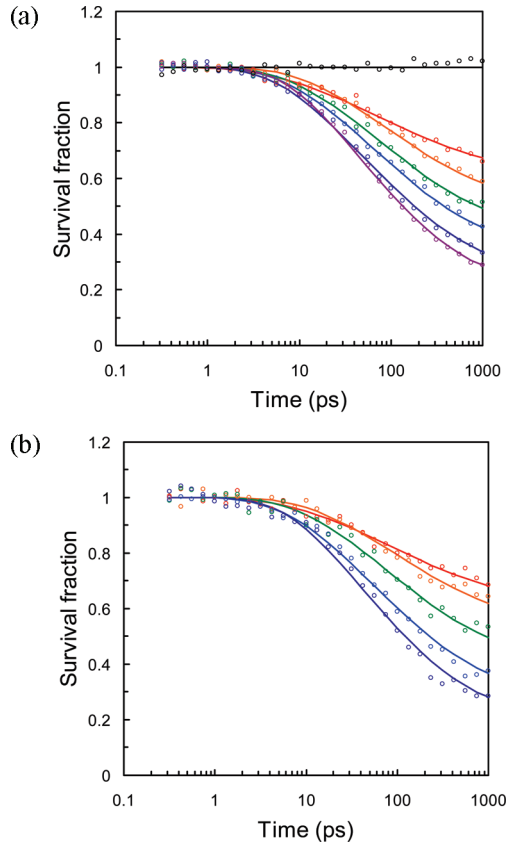

Figure 4. (a) Kinetics of survival fraction of deligated heme in MpCO in D_2O and glycerol/water mixtures at 294 K after photolysis. The viscosity of the sample was adjusted by varying glycerol content in the glycerol/water mixture. The solid lines are the fit to the theory of diffusion-controlled reaction (see text). (b) Kinetics of survival fraction of deligated heme in MpCO in 85% glycerol/water at 283, 293, 303, 313, and 323 K. Viscosity of the solution is 223, 109, 58, 33.5, 21 cP from low to high temperatures. The solid lines are fit to the theory of diffusion-controlled reaction.

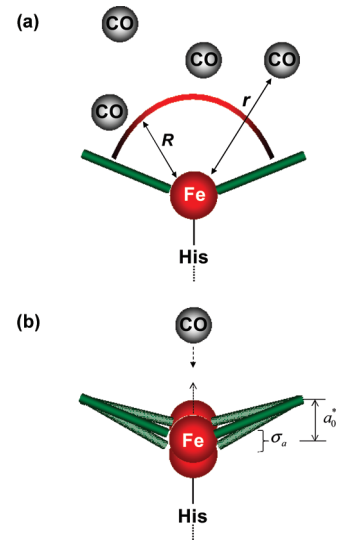

Figure 5. Illustration for the diffusion model (a) and the SRC model (b) used in the text. Thick green lines represent the cross section of the porphyrin plane and gray spheres various positions of CO. His: proximal histidine; Fe: iron atom; R: the reaction radius; r: the distance of the initial separation of CO and Fe after photodissociation; a_0* and σ_a: average out-of-plane displacement of the iron in the deligated Mp and its standard deviation.

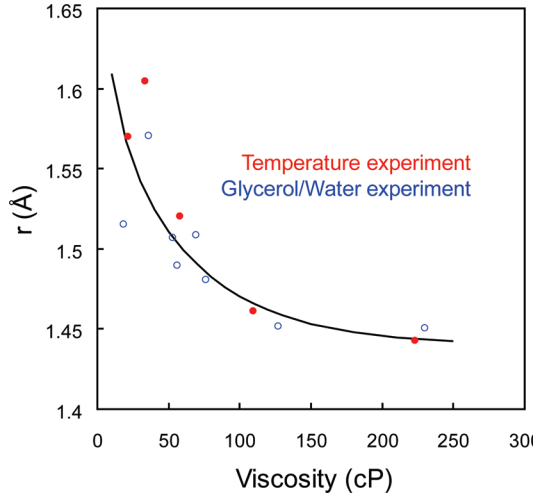

Figure 6. Viscosity-dependent initial separations in the diffusion model recovered from the fit. One is obtained by varying the glycerol content in the glycerol/water mixture (blue open circles) and the other by changing temperature (red filled circles). The solid line serves as a guide to the eye.

reaction radius. For spherically symmetric diffusion, $k_D = 4\pi RD$. Here, since CO reacts only from the distal side of the heme plane, a reactive hemisphere protruding from an infinite reflecting plane (Figure 5a) was assumed and thus k_D was set to $2\pi RD$.[27,45] Four parameters (D, R, r, k_0) were required to describe $W(t)$. It is reasonable to consider R as an intrinsic property of the CO reaction in Mp and is assumed independent of the solution viscosity at 294 K and any temperature in the range of 283−323 K explored in this experiment. Since the diffusion coefficient was inversely proportional to the viscosity of the solution, one global D was enough to fit the whole set of kinetic traces to various viscosity solutions. With global R and D, k_0 was found to be independent of the sample conditions and thus was treated as a global parameter. When the kinetic traces of various glycerol/water mixtures at 294 K (8 kinetic traces) and those in 85% glycerol/water mixture at various temperatures (5 kinetic traces) were separately fit, the recovered global parameters (D, R, k_0) from both fittings were nearly identical. Therefore, in the final fitting, we optimized three global parameters (D, R, k_0) and one local parameter (r) by simultaneously fitting 13 kinetic traces of the survival fraction. As seen in Figure 4, the kinetics of the survival fractions at various viscous solutions were well described by $W(t)$. The recovered parameters from the global fitting were the following: $R = 1.36$ Å; $k_0 = 4.1 \times 10^{-14}$ cm^3/s; $D = 5.67 \times 10^{-7}$ cm^2/s in 18 cP solution; and $r = 1.45-1.53$ Å. The distance for the initial separation was found to be inversely proportional to the viscosity of the solution (Figure 6).

The kinetics of the survival fraction of the deligated Mp ($f(t)$) was also modeled by the distributed linear coupling model (the SRC model).[29,31] In the SRC model, the kinetics of the survival fraction was expressed by three parameters (C, E, t_0):[29]

$$f(t) = \int_0^\infty dx \, \frac{C}{2\sqrt{\pi x}} \left(e^{-(C\sqrt{x} - E)^2} + e^{-(C\sqrt{x} + E)^2}\right) e^{-t/t_0 e^{-x}} \quad (2)$$

$$C \equiv \sqrt{\frac{k_B T}{\kappa {\sigma_a}^2}}, \quad E \equiv \frac{1}{\sqrt{2}} \frac{{a_0}^*}{\sigma_a}, \quad t_0 \equiv \frac{e^{H_0/k_B T}}{A_0}$$

where a_0* is the average Fe out-of-plane coordinate displacement in the deligated Mp and σ_a is its standard deviation (Figure 5b), κ is the effective force constant associated with moving the Fe into the heme plane, k_B is the Boltzmann constant, and A_0 is the Arrhenius prefactor in the expression for the rebinding rate: $A_0 \exp(-H/k_B T)$.[29] In this model, the enthalpic barrier for CO rebinding (H) was separated into the proximal barrier due to heme doming (H_p), and the remaining (mostly distal) barrier (H_0, (i.e., $H = H_p + H_0$)). Three independent parameters (C, E, t_0) were optimized by fitting the kinetics of the survival fraction. The physical parameters at each sample condition were then obtained as follows:[29]

$$a_0^* = \sqrt{\frac{2k_B T}{\kappa}}\left(\frac{E}{C}\right), \quad \sigma_a = \sqrt{\frac{k_B T}{\kappa C^2}}, \quad \bar{H}_p = k_B T\left(\frac{E}{C}\right)^2 \tag{3}$$

$$-\log(t_0) = \log(A_0) - \frac{H_0}{k_B T \ln 10} \tag{4}$$

In Figure 7, the values of a_0* and σ_a were plotted as a function of the viscosity of the solution, recovered from the kinetics of the survival fraction of the deligated Mp. In calculating these quantities, the doming force constant κ was taken to be 13.8 N/m,[31] the value for Mb and cytochrome *c*. The recovered parameters were the following: a_0* = 0.37−0.72 Å; σ_a = 0.17−0.38 Å; and $\bar{H}_p$ = 6−22 kJ/mol. Larger force constants of 27.6 N/m[29] were used in obtaining parameters for the kinetics of H_2O-FePPIX-CO.[29] The larger value will decrease a_0* and σ_a by a factor of 1.414. We obtained H_0 and A_0 by plotting temperature-dependent values of $-\log(t_0)$ versus $1/T$ as in eq 4. Due to the limited temperature range in the data, only the range of the values can be extracted: H_0 = 0−1.4 kJ/mol and $A_0 = 0.8 \times 10^{11}$−1.3×10^{11} s^{-1}. These values are similar to those of H_2O-FePPIX-CO, where H_0 = 0 kJ/mol and $A_0 = 1.5 \times 10^{11}$ s^{-1}.

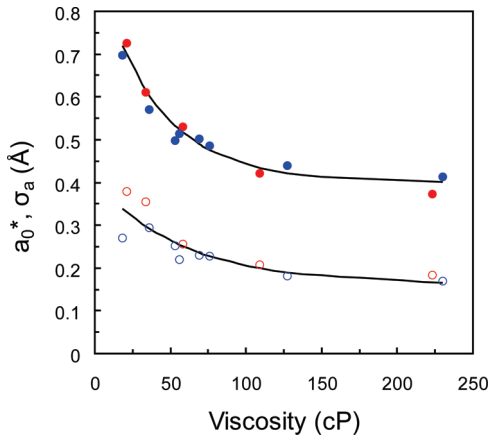

Figure 7. Viscosity-dependent average out-of-plane displacement of the iron (filled circle) in the deligated state and its standard deviation (open circles) recovered from the fit. Viscosity was adjusted either by varying glycerol composition in the glycerol/water mixture (blue symbols) or by varying temperature (red symbols).

Discussion

The Fe−CO bond energy in the heme molecule (~23 kcal/mol[46,47]) is much smaller than the energy of the excitation photon, 575 nm (49.6 kcal/mol), and thus, an excess of energy can be deposited into the dissociated CO during photolysis of Fe−CO in MpCO. The CO with excess kinetic energy can fly away from the Fe atom. However, according to MD simulations on the photodissociation of MbNO,[48] the excess kinetic energy of the dissociated ligand is thermalized within 300 fs and the dissociated ligand assumes diffusive motion shortly after photodissociation. Like NO in MbNO, the dissociated CO from MpCO likely starts to diffuse shortly after photolysis and the diffusive motion will make the dissociated CO drift away from the Fe atom. The more diffusive the ligand is, the more rapidly it spreads away from the Fe atom. The diffusive motion is dictated by the viscosity of the solution. Since the ligand in a higher viscosity solution will diffuse more slowly, it stays near the Fe atom for a longer period of time. As seen in Figure 4, the geminate yield of CO rebinding to Mp increased and its rate accelerated as the viscosity of the solution increased either by increasing glycerol content in the glycerol/water mixtures at 294 K or by decreasing the temperature of the solution from 323 to 283 K, which clearly suggested that retention of the dissociated CO near the heme for a longer period by the viscous solvent media accelerated rebinding.[28] It is consistent with faster and more efficient geminate rebinding of CO to cytochrome *c* than Mp,[49] where the organized protein matrix served as an efficient trap for diffusing CO.

Viscosity-dependent nonexponential geminate rebinding of CO to Mp after photolysis of MpCO is well described by the diffusion model, even we assumed that R and k_0 were independent of the solution viscosity at 294 K and independent of temperature in the range of 283−323 K. Note that the survival probability function $W(t)$ does not have an explicit temperature or viscosity dependence; the dependence was reflected in the diffusion coefficient. Here, R and k_0 were obtained by simultaneously fitting 13 sets of kinetic traces as global parameters and thus the fitted values for the parameters were quite robust.

Szabo and co-workers have used the diffusion model to fit the rebinding of CO to H_2O-FePPIX after photolysis of the CO bound heme at 240, 260, 280, and 300 K, measured between 2 ps and 10 ns.[27] In their model, the geminate pair was assumed to be in a contact radius of R (r was set to be equal to R). The function for the survival fraction $S(t)$ in their model could be obtained by substituting r with R in the survival probability function shown in eq 1, resulting in eq 4 in ref 27: $S(t) = W(t;r{=}R) = 1 + [k_0/(k_0 + k_D)]\Omega(A\sqrt{t}) = [k_0 k_D/(k_0 + k_D)]\{1 + (k_0/k_D)\ \exp(\tau)\ \mathrm{erfc}(\sqrt{\tau})\}$, where $\tau = [Dt/R^2][(k_0 + k_D)/k_0]^2$. Fitting their data to this equation, they found that contact radius R was temperature-independent 1.5 Å and $k_0 = 4.2 \times 10^{-14}$−$5.4 \times 10^{-14}$ cm^3/s in 240−300 K. Whereas these values were similar to the fitted values reported herein, our data cannot be reproduced by their model. When we tried to fit our data to $S(t) = W(t;r{=}R)$, the fit severely deviated from the data, in particular, for high-viscosity solutions. Moreover, a close look at their fit also revealed a deterioration in the quality of the fit as the viscosity of the solution increased with decreasing temperature (Figure 2 in ref 27). Clearly, allowing independent initial separation (r), different from the reaction radius (R), was necessary for successful modeling of CO rebinding to the model heme in viscous solutions, suggesting that the CO had moved away from the contact radius by the time it was thermalized.

The MpCO molecule can assume various conformational substates that have different values of R or k_0.[2] Even if MpCO

is in an inhomogeneous mixture of conformational substates, each with a unique R or k_0, an average value of R or k_0 was enough to describe the rebinding kinetics if the interconversion between conformational substates was fast enough. The successful fitting of the presented data by the diffusion model using a single value of R or k_0 suggested that the interconversion was faster than the geminate rebinding of CO to Mp in a solution of glycerol/water at 283−323 K.[27] It was consistent with the previous conclusions that the interconversion between the substates of H_2O-FePPIX was sufficiently fast between 240 and 300 K, and that the nonexponential geminate rebinding could be attributed to the diffusion of the ligand.[27] If MpCO had various conformations with different rebinding parameters, the recovered parameters from the fit should be interpreted as average values of the distribution of the corresponding values.

The fitted value of the reaction radius, $R = 1.36$ Å, was shorter than the Fe−C bond length of ∼1.8 Å.[27,50] The distance between the Fe and center of the CO molecule should be larger than the Fe−C bond length. However, the CO molecule can bind to Fe not only when it is within bonding distance, but also in a proper orientation for Fe−CO bond formation.[27,50] In other words, all CO molecules within the reaction radius cannot bind to Fe due to orientational constraints imposed by the geometry of the Fe−CO bond, resulting in a smaller reaction radius when the molecular orientation was not considered. The recovered value for MpCO was similar to the fitted value of $R = 1.5$ Å for H_2O-FePPIX-CO using the diffusion model.

For H_2O-FePPIX-CO, the intrinsic rate constant at reaction radius was found to be weakly dependent on temperature and has been estimated from low-temperature data. The value of 5.6×10^{-14} cm^3/s at 300 K was calculated by using $k_0 = k \cdot 2\pi R^3/3$, in the limit that the distribution of the rate constant was independent of temperature and the interconversion among substates sufficiently fast.[27] In the calculation, the average rate constant of $k = 8 \times 10^9$ s^{-1} was extrapolated from the low-temperature data[26,27] and the fitted value of $R = 1.5$ Å. The estimated value was nearly identical to the fitted value of 5.4×10^{-14} cm^3/s for H_2O-FePPIX-CO at 300 K. Within the same assumption used for the above calculation of the intrinsic rate constant at reaction radius, the calculated k_0 with use of $R = 1.36$ Å, instead of 1.5 Å, was 4.2×10^{-14} cm^3/s, which is within experimental error, identical to the presented fitted value of $k_0 = 4.1 \times 10^{-14}$ cm^3/s.

Since the Fe atom is a part of the Mp molecule, its diffusion can be negligible during geminate rebinding. Therefore, the sum of the diffusion coefficients of Fe and CO (D) can be approximated to the diffusion coefficient of CO. The fitted value of $D = 5.7 \times 10^{-7}$ cm^2/s in an 18 cP solution was consistent with the calculated value of CO in glycerol/water at 294 K (6.0×10^{-7} cm^2/s), using Stokes' law ($D = k_B T/6\pi\eta\sigma$), where σ is the hard sphere radius of CO, deduced to be 2.0 Å.[27]

One noticeable finding from the presented analysis was that the initial separation between CO and Fe was inversely proportional to solution viscosity. The value of r could be considered the distance between CO and Fe when the photolyzed CO was thermalized. Initially, the departing CO after photolysis, which has an excess kinetic energy, would collide with surrounding solvent molecules, lose initial kinetic energy, and assume diffusive motion as it was thermalized. Viscosity-dependent r implied that collision with a more viscous solvent was more efficient in losing excess kinetic energy and thus, the loss of the initial kinetic energy faster, resulting in a shorter value of r for the dissociated CO in higher viscosity solvent. It can also be viewed as the dissociated CO traveled less distance in a given time at higher viscosity solution.

The kinetics of the rebinding of CO to Mp after photolysis of MpCO in viscous solution is well described by the three-parameter SRC model (eq 2), from which the fundamental parameters of a_0*, σ_a, H_0, and A_0 are calculated. The SRC model assumed that heme doming takes place on a femtosecond time scale[13,51] and that the nonexponential CO rebinding arises from a heterogeneous distribution of heme conformations (mostly the Fe out-of-plane displacement), fluctuational averaging of which takes place slower than CO rebinding.[29] If the averaging occurred faster than the ligand rebinding, the kinetics of CO rebinding would be exponential.[29] The rate of solvent structural relaxation, which dictates the fluctuational averaging, could be measured with specific heat capacity and viscosity data, and its time scale estimated to be 100 ps at 313 K and ∼1 ns at 283 K.[52] These time constants were slower than the CO rebinding rate at corresponding temperatures and thus lead to nonexponential CO rebinding to Mp as observed. Nonexponential ligand rebinding can arise from slow relaxation as well as a heterogeneous distribution of heme conformations.[53] Whereas the heme doming process of Mb was reported to stretch from hundreds of picoseconds to nanoseconds,[54−56] that of the bare heme was suggested to take place on subpicosecond time scales.[29] Therefore, the nonexponential CO rebinding to Mp could be attributed not to slow relaxation, but to the heme structural distribution. The SRC model has successfully modeled temperature-dependent kinetics of CO rebinding to H_2O-FePPIX in 80% (v/v) glycerol/water.[29] It was found that the Fe out-of-plane displacement increased from 0.08 to 0.27 Å, and that its standard deviation increased from 0.06 to 0.11 Å as temperature increased from 40 to 290 K.[29] For CO binding to Mp, we obtained the values of a_0* = 0.37−0.72 Å and σ_a = 0.17−0.38 Å in the temperature range of 283−323 K. Both values increased as temperature increased or as viscosity decreased (see Figure 7), indicating that the Fe out-of-plane displacement and its standard deviation of Mp are larger in lower viscosity solution. It is consistent with the larger Fe displacement observed in H_2O-FePPIX at higher temperature. The recovered a_0* and σ_a of Mp are much larger than those of H_2O-FePPIX, suggesting that bonding of the proximal histidine to Fe atom requires larger Fe displacement away from the heme plane and broader distribution in the displacement. The extracted proximal barrier of $\bar{H}_p$ = 6−22 kJ/mol for MpCO was higher than 6 kJ/mol for H_2O-FePPIX-CO at room temperature due to larger Fe out-of-plane displacement, but the distal barrier and the Arrhenius prefactor were similar to those for H_2O-FePPIX-CO.

Figure 8 shows the temperature-dependent, first two moments of the heme geometry distribution for Fe out-of-plane displacement of heme molecules after photolysis of the bound CO. Values at 40−290 K are for H_2O-FePPIX[29] and those at 283−323 K for Mp after photolysis. The values for MbCO at low temperature and CO bound cytochrome c at room temperature[49] were also given for comparison. Whereas the tendency of both values of Mp with varying temperature is an acceptable range of those of H_2O-FePPIX, the magnitude of the displacement and the standard deviation appears to be too large. The Fe out-of-plane displacement and its standard deviation of Mp can sharply increase with temperature above 283 K but these values could have been overestimated due to the limitation of the SRC model. Since diffusive motion of the dissociated ligand gets more important with increasing temperature, it can play a more significant role in the rebinding of the dissociated CO. Therefore, the SRC model, attributing the nonexponential

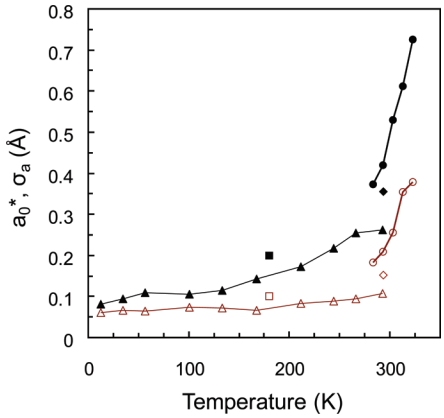

Figure 8. Temperature-dependent average out-of-plane displacement of Fe in the deligated state (filled symbols) and its standard deviation (open symbols) recovered from the fit. Parameters for H_2O-FePPIXCO (triangles),[29] MbCO (squares),[31,57] CytcCO (rhombuses),[49] and MpCO (circles) are shown for comparison.

rebinding of CO to the distribution of the Fe out-of-plane displacement alone, may result in the overestimated a_0* and σ_a in high temperature where diffusion of the ligand is significant (vide infra).

Band III is known to be sensitive to the position of the Fe out-of-plane displacement in the heme.[7,55] Champion and co-workers found that band III of H_2O-FePPIX shifted from 773 to 781.5 nm as temperature increased from 170 to 290 K. This observed red shift was used as evidence for the larger value of a_0* at higher temperatures. According to the above reasoning, since the extracted a_0* for Mp was the largest at the lowest viscosity solution at room temperature, band III of Mp should shift red as the viscosity of the solution decreases. However, we found a slight blue shift in band III of Mp with decreasing viscosity of the solution at room temperature (data not shown). Clearly, the smaller a_0* of Mp in a higher viscosity solution was inconsistent with the larger Fe out-of-plane displacement expected from the position of band III in Mp.

Exponential rebinding of CO to 2-MeIm-FePPIX (the rebinding time constant of 7.7×10^{-10} s at 252 cP solution[28]) was explained by the CO rebinding that proved slower than the structural relaxation of the heme distribution, which was used to justify the validity of the SRC model.[29] It can be successfully modeled with the diffusion model by using the same fitting parameters as MpCO, except with an 8-fold slower intrinsic rate. Imidazole-coordinated FePPIX is known to have a higher rebinding barrier than H_2O-coordinated FePPIX.[30] A higher rebinding barrier leads to slower rebinding, resulting in a smaller intrinsic rate (k_0) in the diffusion model. Exponential rebinding of NO to the model heme was used to argue that the nonexponential rebinding of CO to the model heme was due neither to ligand diffusion nor to heme relaxation.[29] Temperature-independent exponential kinetics of NO rebinding to H_2O-FePPIX was described by a "harpoon" model based on the extra unpaired NO electron.[32] The harpoon model is based on the attractive interaction between reacting molecules.

To describe the validity of the diffusion model, we have tried to fit the kinetics of NO rebinding to Mp using eq 1 ($W(t)$). Equation 1 can fit the early part of the kinetics but fails to reproduce the later part due to a diffusive kinetics at later times in the model not present in the observed NO kinetics. As suggested in the harpoon model, a successful description of the rebinding of NO to a model heme required an attractive interaction between reacting molecules. Therefore, it is not surprising that the NO rebinding kinetics could not be reproduced by $W(t)$, the pair survival probability function *in the absence of any interaction potential between the pair*. The NO rebinding kinetic may be reproduced by the diffusion model if $W(t)$ was modified to accommodate an attractive interaction between two reacting molecules as suggested in the harpoon model. Attractive interaction between the dissociated NO and the Fe atom may result in ultrafast exponential rebinding kinetics almost independent of the solvent viscosity. Unfortunately, the analytical form of the pair survival probability function *in the presence of the interaction potential between the pair* is not yet available to test this presumption.

In the SRC model, nonexponential rebinding kinetics mainly arises from the distribution of the proximal barrier that stems from the distribution of the Fe out-of-plane displacement.[29,31] In this model, the distal barrier can attribute to the rebinding, but distribution in the distal barrier is not considered. In the diffusion model, the nonexponential rebinding kinetics mainly arose from the diffusion of the ligand to the Fe atom.[45] The inhomogeneity of the proximal barrier was not considered and only its average value recovered as the intrinsic rate at contact. In reality, the nonexponential kinetics may arise from both the distribution of the proximal barrier and diffusion of the ligand. When we tried to model the nonexponential kinetics, considering either the distribution of the proximal barrier or the diffusion of the ligand, the overestimated parameters could be recovered for a real system with both contributions.

Conclusions

Viscosity-dependent CO rebinding kinetics to Mp after photolysis of MpCO in glycerol/water mixtures near room temperature were probed with time-resolved vibrational spectroscopy. The rebinding kinetics was highly nonexponential and the geminate rebinding rate and geminate yield higher as the viscosity of the solvent increased. Since the dissociated CO in more viscous media stays longer in the vicinity of the Fe atom, the more efficient rebinding likely arose from the longer retention of CO by the viscous media. The nonexponential rebinding kinetics of CO could be explained by either diffusion of the ligand or an inhomogeneous distribution of the rebinding barrier due to the Fe out-of-plane displacement. The ligand rebinding to Mp cannot exclude either model. On the contrary, the nonexponentiality may have contributions from both the diffusion of the ligand and the distribution of the rebinding barrier.

Acknowledgment. This work was supported by the Midcareer Research Program through an NRF grant funded by the MEST (No. 2007-0056301). The authors would like to thank Professor M. Tachiya for introducing the diffusion model and Professor H. Kim for helpful discussions on the diffusion model.

References and Notes

(1) Antonini, E.; Brunori, M. *Hemoglobin and Myoglobin in Their Reactions With Ligands*; North-Holland Publishing Company: London, UK, 1971.

(2) Austin, R. H.; Beeson, K. W.; Eisenstein, L.; Frauenfelder, H.; Gunsalus, I. C. *Biochemistry* **1975**, *14*, 5355.

(3) Springer, B. A.; Sligar, S. G.; Olson, J. S.; Phillips, G. N., Jr. *Chem. Rev.* **1994**, *94*, 699.

(4) Ansari, A.; Berendzen, J.; Braunstein, D. K.; Cowen, B. R.; Frauenfelder, H.; Hong, M. K.; Iben, I. E. T.; Johnson, J. B.; Ormos, P.; Sauke, T. B.; Scholl, R.; Schulte, A.; Steinbach, P. J.; Vittitow, J.; Young, R. D. *Biophys. Chem.* **1987**, *26*, 337.

(5) Frauenfelder, H.; Parak, F.; Young, R. D. *Annu. Rev. Biophys. Biophys. Chem.* **1988**, *17*, 451.

(6) Frauenfelder, H.; Sligar, S. G.; Wolynes, P. G. *Science* **1991**, *254*, 1598.
(7) Steinbach, P. J.; Ansari, A.; Berendzen, J.; Braunstein, D.; Chu, K.; Cowen, B. R.; Ehrenstein, D.; Frauenfelder, H.; Johnson, J. B.; Lamb, D. C. *Biochemistry* **1991**, *30*, 3988.
(8) Nienhaus, G. U.; Mourant, J. R.; Frauenfelder, H. *Proc. Natl. Acad. Sci. U.S.A.* **1992**, *89*, 2902.
(9) Ansari, A.; Jones, C. M.; Henry, E. R.; Hofrichter, J.; Eaton, W. A. *Science* **1992**, *256*, 1796.
(10) Balasubramanian, S.; Lambright, D. G.; Marden, M. C.; Boxer, S. G. *Biochemistry* **1993**, *32*, 2202.
(11) Cornelius, P. A.; Steele, A. W.; Chernoff, D. A.; Hochstrasser, R. M. *Proc. Natl. Acad. Sci. U.S.A.* **1981**, *78*, 7526.
(12) Dantsker, D.; Samuni, U.; Friedman, J. M.; Agmon, N. *Biochim. Biophys. Acta, Proteins Proteomics* **2005**, *1749*, 234.
(13) Franzen, S.; Bohn, B.; Poyart, C.; Martin, J. L. *Biochemistry* **1995**, *34*, 1224.
(14) Frauenfelder, H.; Wolynes, P. G. *Science* **1985**, *229*, 337.
(15) Henry, E. R.; Sommer, J. H.; Hofrichter, J.; Eaton, W. A. *J. Mol. Biol.* **1983**, *166*, 443.
(16) Kholodenko, Y.; Gooding, E. A.; Dou, Y.; Ikeda-Saito, M.; Hochstrasser, R. M. *Biochemistry* **1999**, *38*, 5918.
(17) Lim, M.; Jackson, T. A.; Anfinrud, P. A. *JBIC, J. Biol. Inorg. Chem.* **1997**, *2*, 531.
(18) Braunstein, D. P.; Chu, K.; Egeberg, K. D.; Frauenfelder, H.; Mourant, J. R.; Nienhaus, G. U.; Ormos, P.; Sligar, S. G.; Springer, B. A.; Young, R. D. *Biophys. J.* **1993**, *65*, 2447.
(19) Li, H.; Elber, R.; Straub, J. E. *J. Biol. Chem.* **1993**, *268*, 17908.
(20) Petrich, J. W.; Lambry, J.-C.; Balasubramanian, S.; Lambright, D. G.; Boxer, S. G.; Martin, J. L. *J. Mol. Biol.* **1994**, *238*, 437.
(21) Walda, K. N.; Liu, X. Y.; Sharma, V. S.; Magde, D. *Biochemistry* **1994**, *33*, 2198.
(22) Beece, D.; Eisenstein, L.; Frauenfelder, H.; Good, D.; Marden, M. C.; Reinisch, L.; Reynolds, A. H.; Sorensen, L. B.; Yue, K. T. *Biochemistry* **1980**, *19*, 5147.
(23) Martin, J. L.; Migus, A.; Poyart, C.; Lecarpentier, Y.; Astier, R.; Antonetti, A. *Proc. Natl. Acad. Sci. U.S.A.* **1983**, *80*, 173.
(24) Moore, J. N.; Hansen, P. A.; Hochstrasser, R. M. *Chem. Phys. Lett.* **1987**, *138*, 110.
(25) Petrich, J. W.; Poyart, C.; Martin, J. L. *Biochemistry* **1988**, *27*, 4049.
(26) Miers, J. B.; Postlewaite, J. C.; Cowen, B. R.; Roemig, G. R.; Lee, I. Y. S.; Dlott, D. D. *J. Chem. Phys.* **1991**, *94*, 1825.
(27) Miers, J. B.; Postlewaite, J. C.; Zyung, T.; Chen, S.; Roemig, G. R.; Wen, X.; Dlott, D. D.; Szabo, A. *J. Chem. Phys.* **1990**, *93*, 8771.
(28) Lee, T.; Park, J.; Kim, J.; Joo, S.; Lim, M. *Bull. Korean Chem. Soc.* **2009**, *30*, 177.
(29) Ye, X.; Lonascu, D.; Gruia, F.; Yu, A.; Benabbas, A.; Champion, P. M. *Proc. Natl. Acad. Sci. U.S.A.* **2007**, *104*, 14682.
(30) Ye, X.; Yu, A.; Georgiev, G. Y.; Gruia, F.; Ionascu, D.; Cao, W.; Sage, J. T.; Champion, P. M. *J. Am. Chem. Soc.* **2005**, *127*, 5854.
(31) Srajer, V.; Reinisch, L.; Champion, P. M. *J. Am. Chem. Soc.* **1988**, *110*, 6656.
(32) Ye, X.; Yu, A.; Champion, P. M. *J. Am. Chem. Soc.* **2006**, *128*, 1444.
(33) Aron, J.; Baldwin, D. A.; Marques, H. M.; Pratt, J. M.; Adams, P. A. *J. Inorg. Biochem.* **1986**, *27*, 227.
(34) Kim, S.; Jin, G.; Lim, M. *J. Phys. Chem. B* **2004**, *108*, 20366.
(35) Lim, M.; Wolford, M. F.; Hamm, P.; Hochstrasser, R. M. *Chem. Phys. Lett.* **1998**, *290*, 355.
(36) Hamm, P.; Kaindl, R. A.; Stenger, J. *Opt. Lett.* **2000**, *25*, 1798.
(37) Hamm, P.; Lim, M.; Hochstrasser, R. M. *J. Phys. Chem. B* **1998**, *102*, 6123.
(38) Urry, D. W.; Pettegrew, J. W. *J. Am. Chem. Soc.* **1967**, *89*, 5276.
(39) Cao, W.; Ye, X.; Georgiev, G. Y.; Berezhna, S.; Sjodin, T.; Demidov, A. A.; Wang, W.; Sage, J. T.; Champion, P. M. *Biochemistry* **2004**, *43*, 7017.
(40) White, W. I. *The Porphyrins*; Academic Press: New York, 1978; Vol. 5.
(41) Lide, D. R. *CRC Hanbook of Chemistry and Physics*, 76th ed.; CRC Press, Inc.: Boca Raton, FL, 1995.
(42) Lim, M.; Jackson, T. A.; Anfinrud, P. A. *J. Chem. Phys.* **1995**, *102*, 4355.
(43) Kim, H.; Shin, S.; Shin, K. J. *J. Chem. Phys.* **1998**, *108*, 5861.
(44) Tachiya, M. *Radiat. Phys. Chem.* **1983**, *21*, 167.
(45) Shoup, D.; Lipari, G.; Szabo, A. *Biophys. J.* **1981**, *36*, 697.
(46) Mills, F. C.; Ackers, G. K.; Gaud, H. T.; Gill, S. J. *J. Biol. Chem.* **1979**, *254*, 2875.
(47) Rudolph, S. A.; Boyle, S. O.; Dresden, C. F.; Gill, S. J. *Biochemistry* **1972**, *11*, 1098.
(48) Meuwly, M.; Becker, O. M.; Stote, R.; Karplus, M. *Biophys. Chem.* **2002**, *98*, 183.
(49) Kim, J.; Park, J.; Lee, T.; Lim, M. *J. Phys. Chem. B* **2009**, *113*, 260.
(50) Marden, M. C. Ph.D. Thesis, University of Illinois, 1980.
(51) Ye, X.; Demidov, A.; Rosca, F.; Wang, W.; Kumar, A.; Ionascu, D.; Zhu, L.; Barrick, D.; Wharton, D.; Champion, P. M. *J. Phys. Chem. A* **2003**, *107*, 8156.
(52) Hayashi, Y.; Puzenko, A.; Feldman, Y. *J. Non-Cryst. Solids* **2006**, *352*, 4696.
(53) Petrich, J. W.; Lambry, J. C.; Kuczera, K.; Karplus, M.; Poyart, C.; Martin, J. L. *Biochemistry* **1991**, *30*, 3975.
(54) Kuczera, K.; Lambry, J. C.; Martin, J. L.; Karplus, M. *Proc. Natl. Acad. Sci. U.S.A.* **1993**, *90*, 5805.
(55) Lim, M.; Jackson, T. A.; Anfinrud, P. A. *Proc. Natl. Acad. Sci. U.S.A.* **1993**, *90*, 5801.
(56) Tian, W. D.; Sage, J. T.; Srajer, V.; Champion, P. M. *Phys. Rev. Lett.* **1992**, *68*, 408.
(57) Srajer, V.; Champion, P. M. *Biochemistry* **1991**, *30*, 7390.

JP1050436